Arsenic and metallic trace elements cycling in the surface water-groundwater-soil continuum down-gradient from a reclaimed mine area: Isotopic imprints

Mahmoud Khaska, Corinne Le Gal La Salle, Lara Sassine, Lise Cary, Olivier Bruguier, Patrick Verdoux

Arsenic and metallic trace elements cycling in the surface water-groundwater-soil continuum down-gradient from a reclaimed mine area: Isotopic imprints

Mahmoud Khaska [a,b,*], Corinne Le Gal La Salle [a,b], Lara Sassine [a,b], Lise Cary [c], Olivier Bruguier [d], Patrick Verdoux [a]

[a] University of Nîmes, EA 7352 CHROME, rue du Dr. Georges Salan, 30021 Nîmes, France
[b] Aix-Marseille University, CNRS IRD-Collège de France, UM 34 CEREGE, Technopôle de l'Arbois, BP80, 13545 Aix-en-Provence, France
[c] BRGM, French Geological Survey, F-59810 Lesquin, France
[d] Montpellier University, UMR CNRS 6250 Géosciences Montpellier, CC 60, Place Eugène Bataillon, 34095 Montpellier Cedex 05, France

ABSTRACT

One decade after closure of the Salsigne mine (SW France), As contamination persisted in surface water, groundwater and soil near and down-gradient from the reclaimed ore processing site (OPS). We assess the fate of As and other associated chalcophilic MTEs, and their transport in the surface-water/groundwater/soil continuum down-gradient from the reclaimed OPS, using Sr-isotopic fingerprinting. The Sr-isotope ratio was used as a tracer of transfer processes in this hydro-geosystem and was combined to sequential extraction of soil samples to evaluate the impact of contaminated soil on the underlying phreatic groundwater. The contrast in Sr isotope compositions of the different soil fractions reflects several Sr sources in the soil. In the complex hydro-geosystem around the OPS, the transport of As and MTEs is affected by a succession of factors, such as (1) Existence of a reducing zone in the aquifer below the reclaimed OPS, where groundwater shows relatively high As and MTEs contents, (2) Groundwater discharge into the stream near the reclaimed OPS causing an increase in As and MTE concentrations in surface water; (3) Partial co-precipitation of As with Fe-oxyhydroxides, contributing to some attenuation of As contents in surface water; (4) Infiltration of contaminated stream water into the unconfined aquifer down-gradient from the reclaimed OPS; (5) Accumulation of As and MTEs in soil irrigated with contaminated stream- and groundwater; (6) Release of As and MTEs from labile soil fractions to underlying the groundwater.

1. Introduction

Tracking the geochemical cycles of metallic trace elements (MTEs) and arsenic in a post mining context is essential for a better orientation of environmental management, remediation strategy and neighborhood protection. Arsenic contamination is a major risk to human health and is a prominent environmental cause of cancer (Smith, 2002). Mining activities involving As ores have an impact on the environment and on human health that may persist for many decades after mine closure (Smedley and Kinniburgh, 2002).

High As concentrations are observed at numerous mining sites (Azcue et al., 1994; Azcue and Nriagu, 1995). In an As-Au mine, the natural occurrence of As is associated with sulfide minerals, especially arsenopyrite (FeAsS), and realgar (AsS) (Cullen and Reimer, 1989; Matschullat, 2000; Moore et al., 1988; Smedley and Kinniburgh, 2002). In addition to mining effluents derived from water treatment, the oxidation of sulfides, such as FeAsS, is a common process, resulting in the release of As into the total environment (surface water, groundwater, soil and sediment) (Basu and Schreiber, 2013). Even after mine decommissioning, As sources remain in the form of tailings dams, dumps, or As-bearing ore stored on site.

Arsenic is among the most problematic and most studied metalloid elements in the environment because of its mobility over a wide range of redox conditions (Smedley and Kinniburgh, 2002). As (III) is the dominant form under reducing and acidic conditions, while As (V) is the prevalent form under oxidizing conditions. In soil, sediment and water, adsorption and desorption are the main processes controlling As transport and fate (Burton et al., 2009;

* Corresponding author at: Univ. Nîmes, EA 7352 CHROME, Rue du Dr. Georges Salan, 30021 Nîmes, Cedex 1, France.
E-mail address: mahmoud.khaska@unimes.fr (M. Khaska).

Deschamps et al., 2005; Dousova et al., 2012; Feng et al., 2013; Garcia-Sanchez and Alvarez-Ayuso, 2003; Mukherjee et al., 2008a; Román Ross et al., 2006; So et al., 2008). Arsenic adsorbs on Fe- and Mn-oxides, carbonates, clay and organic materials (Bardelli et al., 2011; Bauer and Blodau, 2006; Guan et al., 2009; Postma et al., 2010; Román-Ross et al., 2006; So et al., 2008; Song et al., 2006; Yokoyama et al., 2012; Zheng et al., 2004). These processes are controlled by the prevailing physical and chemical context, mainly redox conditions, pH, and temperature (Kelderman and Osman, 2007; Mukherjee et al., 2008a, 2008b; Polizzotto et al., 2006; Robertson, 1989; Xie et al., 2009). Under reducing conditions, the increase of dissolved As is often explained by the dissolution of As-bearing Fe-oxyhydroxide and ferric arsenate (Deuel and Swoboda, 1972; Muehe et al., 2013; Welch and Lico, 1998).

The Salsigne mesothermal Au–As mine (southern France) lies in the southern external zones of the French Variscan orogen (Fig. 1). It was considered as the greatest Au–As mine in France and has been exploited for 96 years. Since the start of mining activities, a considerable amount of As has been transmitted to the environment surrounding the mining and ore-processing areas, either in particulate form (dust), or as dissolved fractions (acid mine drainage), exposing the entire local ecosystem to As contamination. After mine closure, extensive remediation actions were carried out at the reclaimed ore processing site (OPS) (Fig. 1). Nevertheless, As concentrations in surface water and groundwater down-gradient from the reclaimed OPS remain significantly higher than that of the regional background (Khaska et al., 2015).

Dissolved arsenic and MTEs such as Cu, Zn, Co, Ni, Sb, Sn, Cd in soil solution may be transported outside the system by downward mass transfer during floodwater infiltration to deeper soil layers, or even into the underlying aquifer, or by upward mass transfer during plant uptake, or during microbial As-methylation processes producing volatile methylarsines (Casentini et al., 2011; Ravenscroft et al., 2009; Smedley and Kinniburgh, 2002). At the same time, MTEs are involved in chemical reactions occurring in the soil solid phase. MTE concentrations in soil solution are governed by interrelated processes, such as inorganic/organic complexation, oxidation/reduction-, precipitation/dissolution- and adsorption/desorption reactions (Kabata-Pendias, 2004). Predicting the concentration of a given dissolved metallic element in soil solution depends on the accuracy of predictions of changes in soil-environmental conditions over time, such as the degradation of organic matter, changes in pH, redox potential, or the chemical composition of soil solution. Speciation may also evolve accordingly.

Sequential-extraction techniques have been used for characterizing the distribution of metallic elements in the different soil and sediment fractions (Gleyzes et al., 2002; Li and Thornton, 2001), for predicting their mobility (e.g. Aubert et al. 2004); and for determining their origin (Campanella et al., 1995; Tessier et al., 1979). A seven-step sequential extraction procedure was used in this paper on a representative soil sample in order to: i) investigate the distribution of MTE and As contents associated with the different soil fractions, and ii) determine the potential impact of the contaminated soil on unconfined groundwater.

Furthermore, such techniques can be combined with isotopic composition determination, e.g. Pb isotopes (Cary et al., 2015; Teutsch et al., 2001), to distinguish between various possible metal sources. Here, we use the Sr isotopic ratio for tracking the fate of As and other associated chalcophilic MTEs, such as Ni, Cd, Co, Cr, Zn, Cu, Sn and Sb, and their transport mode in the surface-water/groundwater/soil continuum, to assess environmental pollution and human exposure in a post mine closure context. $^{87}Sr/^{86}Sr$ ratio is widely used in pollution studies to track natural and/or anthropogenic processes (Aquilina et al., 2015; Cary et al., 2014; McArthur et al., 2001; Négrel and Petelet-Giraud, 2005; Pennisi et al., 2009). In particular, at this study site Khaska et al. (2015) showed that, $^{87}Sr/^{86}Sr$ ratio is a powerful tool for distinguishing between sources of Sr and As. In this context, Sr isotopes were used as tracers to differentiate the natural and anthropogenic sources of As and other trace elements released from a mining context where CaO is used in the water treatment process. They evidenced the mobilization of As stored in unconfined aquifer to the stream water during dry season, and the mobilization of As with surface runoff during intense rainy events at the vicinity of the reclaimed OPS.

The present study aims to track the fate of As and MTEs down-gradient of the reclaimed OPS in the surface water/groundwater system, and to determine the influence of As and MTE soil contents on the underlying unconfined aquifer. Furthermore, Sr isotopes were coupled to the geochemical composition of the different fractions of the soil, derived from sequential extraction, in order to determine the As and MTE labile fractions.

The objectives of the present study are to:

1. Determine the fate of dissolved As and other MTEs, at the interface between the reclaimed OPS and surface water, between surface water and the Fe-oxyhydroxide film precipitated on the streambed, and in the surface-water-groundwater-soil continuum;
2. Assess the impact of contaminated soil on water quality of the subjacent unconfined aquifer by means of isotopic study and sequential extractions.
3. Study the distribution of As and MTE in the different phases of the contaminated soil, in order to determine the labile soil fraction able to influence the composition of groundwater.

We first discuss the processes of MTE release in association with As in surface water near the reclaimed OPS. Then we assess the mechanism for As and MTE accumulation in the solid phase precipitated from contaminated surface water. Thereafter, the interaction between surface water and groundwater is discussed, the accumulation of As and MTE in soil, as well as the impact of contaminated soil on the underlying aquifer. Finally, we provide a conceptual model showing the mechanism of As transfer into the continuum of surface, groundwater and soil.

2. Geological setting

The study area is located in the southern Massif Central, SW France. On a local scale, the area lies in the southern part of the Orbiel Valley (Fig. 1), 4 km down-gradient from the reclaimed OPS. The lithology of the unconfined aquifer near the reclaimed OPS is described in Khaska et al. (2015). The aquifer matrix mainly consists of Tertiary formations and Quaternary molasse deposits, with a lithologic facies dominated by fluvial sand, loam, clay and carbonate rocks. The heterogeneous aquifer comprises fine to coarse quartz-rich sand with abundant schist material in the shallow part of the aquifer, interbedded with clayey sand and gravel. Gravel is commonly encountered at 3 m below ground surface in the aquifer, and indurated sand forms discontinuous lenses at shallow depth where past water-table fluctuations occurred (Berger et al., 1993). The thickness of the unconfined aquifer is about 10 m on average.

3. Material and methods

Concentrations of minor- and trace-elements were determined for collected water samples (surface water and groundwater) and on solid samples (soil, sequential extraction of As and MTE in the solid soil phase, and Fe-oxyhydroxide film precipitated in the

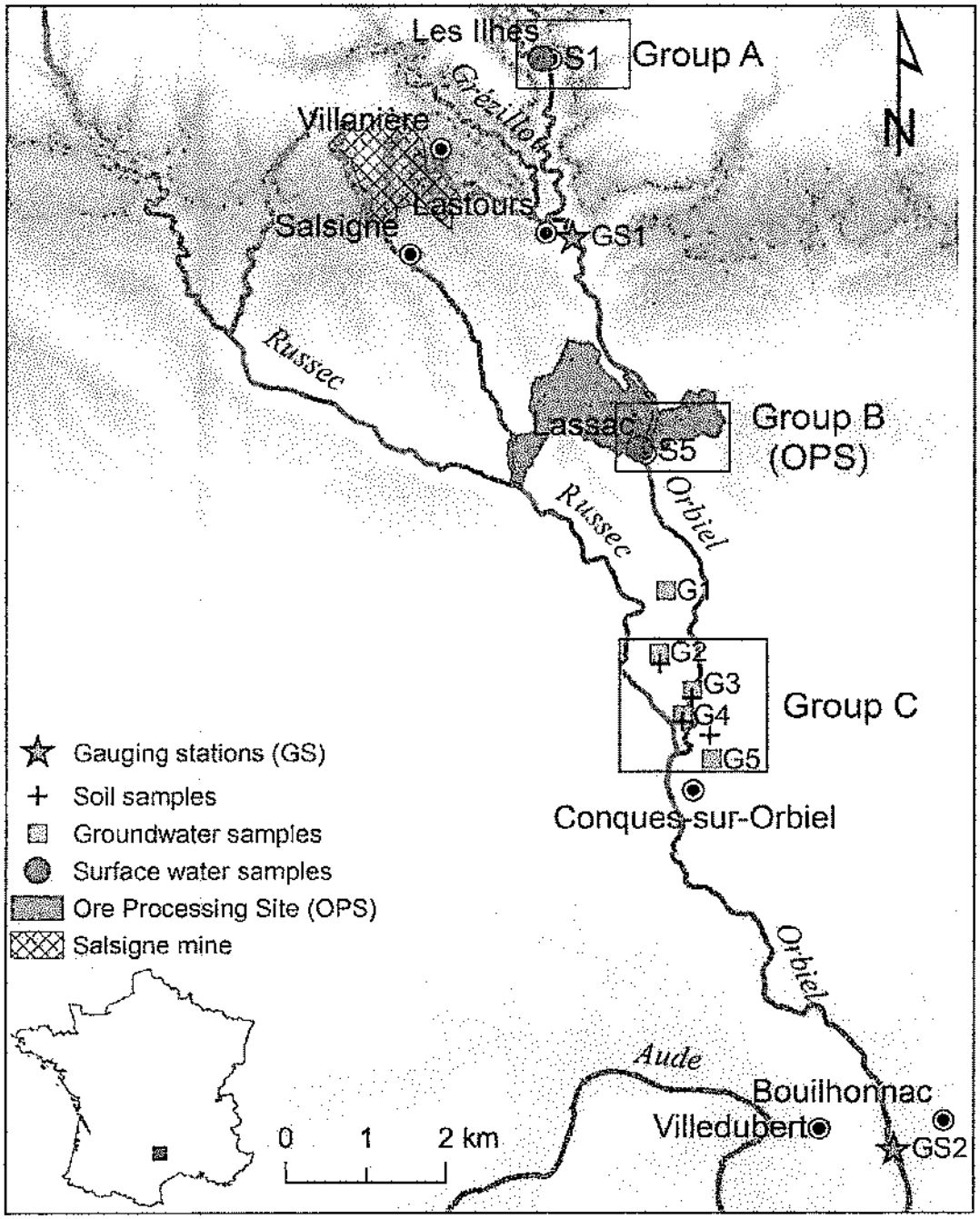

Fig. 1. Schematic map of the study area showing the three water groups, soil-sample and water-sample locations on a digital elevation model background.

streambed). These analyses were combined with isotopic fingerprinting of dissolved strontium ($^{87}Sr/^{86}Sr$ ratio).

3.1. Water and soil sampling

First, groundwater was collected in the wet and dry seasons during one hydrological cycle in 2011 at five different sites (G1–G5) in the unconfined aquifer down-gradient from the reclaimed OPS. Following the preliminary investigation of groundwater and surface water made in 2011 (in wet and dry season) and owing to the interesting results, a monthly basis monitoring of surface water was decided for 2012.

A total of 24 surface water samples were collected at two sites (S1 and S5) for a monthly surface-water survey during a full year from January 2012 to January 2013.

The dominant agricultural soils irrigated with contaminated Orbiel stream water were also sampled. Samples were collected with a stainless-steel scoop, sieved at 1 mm and stored at 4 °C until analysis. For each soil-sampling site, four sub-samples were collected from the surface horizon (0–20 cm). 500 g from each soil sample were pooled and vigorously homogenized to obtain a composite soil sample.

Flow data of the Orbiel stream were extracted from the national HYDRO database (www.hydro.eaufrance.fr); its volumetric flow is monitored both upstream of the reclaimed OPS, at the Lastours

gauging station (GS1), where flow was recorded over a period of ten years from 01/01/2001 to 31/12/2010, and downstream of the reclaimed OPS at the Bouilhonnac gauging station (GS2) from 01/01/2001 to 31/12/2012 (Fig. 1).

3.2. Chemical and microscopic analyses

During the 2011 sampling campaign, the physical and chemical parameters (T, EC, pH and ORP) were measured in the field on raw water in a flow-through cell in order to prevent equilibration with the atmosphere. Before sampling, the domestic wells were flushed until stabilization of the physico-chemical parameters. All water samples were filtered in the field through a 0.45 μm MF-Millipore membrane on a Sartorius poly-carbonate filter holder, then stored below 4 °C in 60 mL HDPE bottles pre-cleaned with hot HNO_3 (10% v/v) and deionized water. The filtered water samples for As, MTE and Sr analyses were acidified to pH 2–3 with ultra-pure 14 N HNO_3. Dissolved As concentrations were measured by ICP-MS after mineralization at the LERES laboratory (EHESP of Rennes), in compliance with the NF EN ISO 15587-1 and NF EN 17294-2 standards of the French accreditation organization COFRAC. The uncertainty for dissolved As analyses was ±22% for concentrations <2 μg/L and ±5% for higher concentrations.

MTEs and Sr concentrations were analyzed at Geosciences Montpellier (AETE Regional facility; University of Montpellier, France) using ICP-MS with a precision of ±5%. Major cation concentrations were analyzed at the LyGeS laboratory (University of Strasbourg) using ICP-AES with a precision of ±5%.

In order to determine As and MTEs concentrations in soil, 500 mg of the composite soil sample was mineralized in a mixture of 8 mL HNO_3 (65% v/v), 5 mL HCl (35% v/v) and 1 mL HF (40% v/v) by microwave-assisted extraction in PFA vessels (ETHOS One, Milestone). In the three-step program, samples were heated to 220 °C for 15 min, maintained at that temperature for 90 min, brought back to 100 °C and finally let to cool to room temperature (Table 2). The extract was then filtered through a 0.45 μm PTFE syringefilter, 1 mL of the supernatant was completely evaporated and the residual fraction was dissolved with diluted HNO_3 (2% v/v) for further analyses with ICP-MS. Coated pebbles with reddish/blackish film were collected from the Orbiel streambed close to the reclaimed OPS and analyzed by environmental scanning electron microscopy (ESEM), on a FEI Quanta FEG 200 coupled to an EDS (X-max 50 mm^2) at the University of Montpellier. The approximate minimum detection limit for As with ESEM is ±0.3 wt% and the uncertainty was ≤1 wt%.

3.3. Sequential extractions

First, to evaluate the mobilization of As and MTEs upon a short water-soil contact as would occur in the field during infiltration of recharge, irrigation water or from flooding events, a leaching was carried out using 1 g of soil sample in 10 mL of deionized water under a constant agitation (24 h).

Then, 1 g of homogenized soil sample was treated following the seven-step extraction scheme (Tessier et al., 1979), for extracting 1) exchangeable ions, 2) carbonate-bound ions, 3) ions bound to Fe and Mn oxides, 4) ions bound to solid-phase organic matter, 5) ions bound to humic substances, 6) ions bound to sulfide minerals and, 7) metals remaining in the residual fraction that are assumed to be incorporated as crystalline material (Table 2). Isotope analysis

Chemical separation of Sr, based on the method described by Pin et al. (2003), was performed at the GIS laboratory (University of Nîmes) with a specific extraction chromatography resin (Sr resin, also known as Sr-spec resin, 50–150 μm particle size, obtained from TrisKem International Bruz, France) under a Class 100 laminar-flow hood in a clean room. The $^{87}Sr/^{86}Sr$ ratios in surface water, groundwater, soil extractions and Fe-oxyhydroxide film samples were measured at the GIS laboratory on a TRITON TI thermal-ionization mass spectrometer. The $^{87}Sr/^{86}Sr$ ratios of standards and samples were i) normalized to $^{86}Sr/^{88}Sr$ ratio = 0.1194 to correct for mass bias, and ii) corrected for possible isobaric ^{87}Rb interference by measuring ^{85}Rb and using the natural $^{87}Rb/^{85}Rb$ ratio = 0.385714. For the entire chemical procedure, the Sr total blank was <1 ng. The internal precision on $^{87}Sr/^{86}Sr$ analyses was around 6×10^{-6} (2σ) and always better than 9×10^{-6}. Over the course of the study, repeated analyses of the NBS987 standard were conducted to test the reproducibility of $^{87}Sr/^{86}Sr$ ratio measurements, giving a mean $^{87}Sr/^{86}Sr$ value of 0.710245 ± 0.000006 (2σ, n = 65).

To investigate the major trends and the interrelationships between MTEs concentrations in the data set, multivariate statistical analysis by Principal Component Analysis (PCA) was performed using XLSTAT software. This method consists in converting a set of variables of observations into a new set of uncorrelated variables (the principal components) to find the common variance within the original variables.

A PCA was performed using 15 variables including major elements (Ca, Na, K, Mg), minor elements (Sr, Ba, Rb), trace elements (As, Co, Cu, Zn, Sb, Pb, U) and Sr isotopic ratios ($^{87}Sr/^{86}Sr$) (Fig. 2B).

The geochemical modeling program PHREEQC Interactive 3.4.0 (Parkhurst and Appelo, 1999), using the LLNL database, was used to support the geochemical observations established with the Sr isotopic tracer. The PHREEQC code is widely used to simulate an important range of aqueous geochemical processes including mixing, speciation, batch-reaction, thermodynamic calculation of water-rocks equilibrium.

4. Results

4.1. Geochemistry of surface water and groundwater

We can distinguish three groups of water, labeled A, B and C (Table 1, Fig. 2). In binary diagrams of Sr *vs* cations and according to the geochemical composition of water the three groups of water are clearly individualized (Fig. 2).

1. Group A corresponds to surface water of the Orbiel collected upstream the reclaimed OPS (Site S1),
2. Group B corresponds to surface water of the Orbiel collected in the vicinity of the reclaimed OPS (Site S5).
   Group C corresponds to groundwater from the phreatic alluvial aquifer located down-gradient from the reclaimed OPS (Sites G1–G5).

This clustering is statistically confirmed by principal component analyses (PCA). Water samples from Group A were characterized by a low mineralization, with total dissolved solids (TDS) ranging from 57 to 115 $mg \cdot L^{-1}$, and being near neutral to slightly alkaline (pH 6.7–7.9). Temperature varied from 10.4 °C to 17 °C (average 13.2 °C) according to the sampling period. Waters from Group B were slightly more mineralized, with TDS ranging from 105 to 143 $mg \cdot L^{-1}$, pH remaining near neutral to slightly alkaline (7.2–7.7) and, temperature ranging from 11.6 to 14.6 °C.

Groundwater from Group C, with a TDS ranging from 215 to 421 $mg \cdot L^{-1}$, was more mineralized than both Groups A and B. The pH values varied between 6.6 and 7.5, and the temperature between 11.2 °C and 16.8 °C with a mean of 15 °C, in agreement with the local average annual temperature. It should be noted that groundwater temperature varies considerably between the dry and the wet seasons, similar to surface water.

Table 1
Metallic trace element and major-cation concentrations for the three groups of water. As and $^{87}Sr/^{86}Sr$ of groups A and B are cited from [illegible]

Groups	Code	Metallic trace elements													Major cations				Sr-isotopes	Physico-chemical parameters			
		Cr	Co	Ni	Cu	Zn	As	Cd	Sb	Pb	U	Si	Fe	Mn	Mg	Ca	Na	K	$^{87}Sr/^{86}Sr$	Eh	PH	T°	EC
		µg L^{-1}													mg L^{-1}					mv		°C	µs/cm
Groups C (2013)	G1	0.5	0.8	1.7	5.8	5.0	6.5	0.14	0.31	0.03	0.6	189	0.005	1.2	15.3	78.5	34.4	1.8	0.71100	437	6.9	14.9	638
	G2	0.2	0.4	2.3	1.1	8.6	39.8	0.07	0.57	0.10	0.2	112	0.012	0.0	9.3	48.7	18.4	1.6	0.71132	277	7.1	15.9	356
	G3	2.2	1.5	4.2	5.1	5.3	39.8	0.92	1.60	0.87	0.4	135	0.021	0.0	9.5	48.2	21.8	1.9	0.71153	377	7.4	13.6	419
	G4	0.6	0.5	1.9	3.5	5.6	24.8	0.06	0.06	0.06	0.2	126	<DL	0.0	9.5	41.8	21.5	1.8	0.71160	507	6.9	16.4	410
	G5	0.9	0.5	2.1	2.6	2.6	10.3	0.06	0.53	0.03	0.3	155	<DL	0.0	11.6	54.3	19.6	1.6	0.71149	364	7.0	16.0	470
	G6	<DL	0.1	<DL	0.5	9.4	16.4	<DL	0.46	0.02	0.2	116	<DL	<DL	9.1	41.1	20.0	1.5	0.71144	273	6.9	15.6	346
	G7	<DL	0.1	<DL	1.4	9.1	12.5	<DL	0.41	0.03	0.3	117	<DL	<DL	8.0	42.8	18.9	1.4	0.71058	302	6.6	16.8	368
	G8	<DL	0.1	<DL	0.5	4.4	11.7	<DL	0.46	0.04	0.4	144	<DL	<DL	11.7	53.8	23.6	1.7	0.71149	457	7.2	13.5	475
	G9	<DL	0.1	<DL	0.3	0.8	10.6	<DL	0.29	0.01	0.2	90	<DL	<DL	6.1	34.6	16.0	1.3		427	7.5	11.2	327
Groups A (2012)	S1	2.0	0.1	0.9	1.3	4.6	2.4	0.01	0.10	0.13	0.06	55	50	4.0	1.4	6.4	5.2	0.8	0.71419	nm	nm	nm	nm
	S2	2.0	0.1	0.8	1.0	4.2	2.5	0.01	0.08	0.15	0.04	34	40	4.0	1.5	7.1	5.5	0.8	0.71436	nm	nm	nm	nm
	S3	2.2	0.1	1.0	2.5	7.4	2.4	0.01	0.68	0.21	0.05	33	36	3.0	1.5	7.2	5.5	1.0	0.71491	nm	nm	nm	nm
	S4	2.0	0.1	1.0	2.0	5.5	2.6	0.01	0.10	0.34	0.09	35	83	3.0	1.5	7.5	5.2	1.0	0.71455	nm	nm	nm	nm
	S5	2.0	0.1	0.8	2.1	6.1	2.9	0.01	0.09	0.01	0.06	40	29	3.0	1.7	8.4	5.6	1.1	0.71471	nm	nm	nm	nm
	S6	2.1	0.1	1.1	3.6	7.6	3.1	0.02	0.09	0.44	0.10	34	155	4.0	1.5	7.4	5.1	0.9	0.71485	nm	nm	nm	nm
	S7	1.9	0.1	1.0	4.4	6.2	3.5	0.03	0.11	0.18	0.03	46	16	4.0	2.1	14.6	6.7	1.6	0.71483	nm	nm	nm	nm
	S8	2.0	0.2	1.1	3.4	8.1	3.2	0.02	0.12	0.63	0.03	52	174	5.0	2.6	13.0	7.9	1.7	0.71489	nm	nm	nm	nm
	S9	1.8	0.1	0.9	2.5	2.4	3.3	0.01	0.09	0.07	0.02	53	4	2.0	2.6	13.0	7.5	1.3	0.71498	nm	nm	nm	nm
	S10	1.9	0.1	0.8	2.3	4.5	3.5	0.01	0.05	0.10	0.02	46	6	3.0	2.4	11.8	7.3	1.7	0.71489	nm	nm	nm	nm
	S11	1.8	0.1	0.7	1.3	1.9	3.0	0.01	0.08	0.26	0.03	44	21	4.0	2.2	10.7	6.3	1.1	0.71510	nm	nm	nm	nm
	S12	2.0	0.1	1.0	2.6	4.7	3.8	0.01	0.07	0.24	0.07	37	79	6.0	1.8	8.4	6.1	1.2	0.71506	nm	nm	nm	nm
	S13	2.1	0.1	0.9	1.9	4.1	2.8	0.01	0.06	0.20	0.04	30	46	3.0	1.5	6.9	5.7	1.0	0.71480	nm	nm	nm	nm
Groups B (2012)	S1	1.8	0.1	0.9	1.5	3.1	14	0.01	0.11	0.20	0.00	43	70	13.0	3.4	14.0	7.2	1.0	0.71400	nm	nm	nm	nm
	S2	2.1	0.2	0.9	1.2	6.3	21	0.01	0.15	0.25	0.10	50	117	27.0	4.4	18.3	10.2	1.9	0.71361	nm	nm	nm	nm
	S3	1.9	0.1	0.9	2.1	9.3	23	0.01	0.13	0.17	0.11	50	101	32.0	4.4	18.9	10.9	1.3	0.71345	nm	nm	nm	nm
	S4	2.0	0.2	1.3	4.4	7.9	24	0.02	0.13	0.29	0.14	56	127	33.0	4.6	19.4	11.9	1.6	0.71411	nm	nm	nm	nm
	S5	1.9	0.1	0.9	1.4	9.5	18	0.01	0.10	0.20	0.11	53	64	19.0	4.3	19.1	9.6	1.1	0.71367	nm	nm	nm	nm
	S6	2.0	0.1	1.4	5.2	7.6	17	0.03	0.13	0.41	0.14	47	138	18.0	3.9	17.3	8.4	1.3	0.71366	nm	nm	nm	nm
	S7	2.0	0.1	1.3	4.6	6.0	48.0	0.02	0.20	0.26	0.15	70	67	28.0	6.4	28.1	10.2	1.7	0.71328	nm	nm	nm	nm
	S8	2.1	0.3	1.6	2.5	6.8	105.3	0.02	0.27	0.17	0.36	194	206	124.0	10.5	44.2	27.8	4.0	0.71285	nm	nm	nm	nm
	S9	2.1	0.3	2.0	5.8	6.9	110	0.02	0.28	0.19	0.30	110	313	110.0	11.6	47.1	28.1	2.4	0.71308	nm	nm	nm	nm
	S10	2.0	0.3	1.5	5.2	5.8	90	0.01	0.23	0.14	0.23	95	206	79.0	9.6	40.0	24.2	2.2	0.71299	nm	nm	nm	nm
	S11	2.0	0.2	1.2	5.4	5.2	48	0.01	0.15	0.22	0.16	70	186	51.0	6.7	29.4	15.0	1.5	0.71310	nm	nm	nm	nm
	S12	2.0	0.2	1.4	3.1	6.7	19.2	0.01	0.14	0.25	0.16	59	89	20.0	5.3	23.4	10.0	1.3	0.71368	nm	nm	nm	nm
	S13	2.0	0.1	1.0	1.3	3.8	20.5	0.01	0.09	0.09	0.11	52	77	22.0	4.8	19.7	10.2	1.3	0.71366	nm	nm	nm	nm

DL: Detection Limit; nm: Not Measured

Table 2
Procedure of sequential extraction, following Tessier et al., (1979) and Compantelli et al. (1995).

Stage	Fraction	Reagents	Conditions	Ratio of Soil: Solution	Agitation	Reaction time (h)
	Sequential extraction					
1	Exchangeable phase	1 M $MgCl_2$	20 °C	1:8	Continuous	1
2	Carbonates phase	1 M HOAc	20 °C	1:8	Continuous	8
3	Fe, Mn oxides phase	0.04 M $NH_2OH.HCl$ in 25% HOAc	75 °C	1:20	Intermittent/Water bath	24
4	Organic matter phase	0.1 M HCl	20 °C	1:8	Continuous	24
5	Humic substances phase	0.5 M NaOH	20 °C	1:8	Continuous	24
6	Sulfides phase	8 M HNO_3	85 °C	1:8	Intermittent/Water bath	3
7	Residual phase	8 mL HNO_3 (65% v/v), 5 mL HCl (35% v/v), 1 mL HF (40% v/v)	220 °C, 900 mbar in AME	1:8		0.7
	Bulk soil	8 mL HNO_3 (65% v/v), 1 mL HF (40% v/v)	220 °C, 900 mbar in AME	1:8		0.7
	Soil H_2O leachate	Ultra pure water (18 MΩ)	20 °C	10	Continual	24

Variations in the oxidation-reduction potential (ORP) of the unconfined groundwater along the Orbiel stream during the dry season showed a net reducing zone in the vicinity of the reclaimed OPS (Khaska et al., 2015). In the current study, the ORP measured upstream and downstream from the reclaimed OPS (Groups A and C) ranged from 0.2 to 0.5 V. This shows that upstream surface water and downstream groundwater from the reclaimed OPS were under moderately to oxidizing conditions (Stumm and Morgan, 1996), in agreement with low concentrations of redox-sensitive elements such as Fe and Mn. In contrast, in the vicinity of the reclaimed OPS, the ORP values of surface water (Group B) were significantly lower, ranging from 0.04 to 0.13 V see Supplementary information (SI), Fig. S1 indicating the presence of a reduced zone (Khaska et al., 2015).

4.2. As and MTE contents in surface and groundwater

The lowest concentrations of As and MTE were observed in surface water upstream from the reclaimed OPS, at site S1 (Group A). They significantly increased at the vicinity of the reclaimed OPS (Group B) (Figs. 3 and 4). Among the measured MTE, only As exceeded the recommended drinking-water standard of 10 $\mu g \cdot L^{-1}$ (WHO, 1996).

Binary diagrams (Fig. 3) show that As, Sb, Ni, Co, U, Ni and Sr concentrations in surface water at the vicinity of the reclaimed OPS at site S5 (Group B) are perfectly correlated with Fe, and Mn concentrations ($0.6 < R^2 < 0.98$) due to a unique source in a context of reduced conditions. Fe and Mn in alluvial groundwater are less than the detection limit of 0.002 and 0.008 $\mu g \cdot L^{-1}$ respectively.

Positive correlations for Group B were also found for As *vs.* Sb, Ni, Co, U and Sr suggesting that these elements were released simultaneously by a single geochemical process, at the OPS. In contrast, the analyzed values for Cd, Cu, Pb and Zn do not correlate with As concentrations, as their concentrations in the vicinity of the reclaimed OPS (site S5) remain within the range of those measured upstream at site S1 (Fig. S2).

The average concentrations of major cations, MTEs and As in groundwater downstream from the reclaimed OPS (Group C) fall within the same range of those observed for surface water at site S5 (Group B), suggesting the influence of surface water on groundwater.

4.3. ESEM analyses of the streambed Fe-oxyhydroxide film

The occurrence of As-bearing Fe-oxyhydroxide precipitate on the streambed at site S5 was indicated by Khaska et al. (2015). Two types of As deposits in pebble coatings were distinguished by ESEM analyses presented in Fig. 4, (i) a regular Fe-oxyhydroxide coating, and (ii) abundant nodules up to 10 μm in size. Arsenic concentrations are twice as high in nodules (4 wt%, n = 8, SD = 0.6 wt%) than in the surrounding Fe-oxyhydroxide coating (2 wt%, n = 12, SD = 1.1 wt%) (Table S1). Low arsenic percentage (~1%) was observed in the uncoated microorganisms (porous diatom silica) (Fig. 4).

4.4. Arsenic and MTE in agricultural soils

The texture of the studied soils is classified as loamy, and the physical, chemical and mineralogical parameters of the soil samples are shown in Table S2. Soil pH is fairly constant, ranging from 7.7 to 8.0 and corresponding to a slightly alkaline soil with low carbonate content. The soil ORP is −35 mV to −20 mV (*vs.* NHE), reflecting moderately reducing conditions. Analytical results of the sequential extraction carried out on the soil samples are given in Table 3 and Fig. 5. All MTE, except As, Zn and Cu, show concentrations below the regional Pedo-Geochemical Baseline (PGB), acquired from the INRA Infosol database (National Institute for Agricultural Research) on a neighboring catchment with similar geological setting, not impacted by mining activities (Table 3). The As concentration in soil (104 $mg \cdot kg^{-1}$) was 3 times higher than the local PGB and 10 times higher than in pristine non-contaminated soils where As contents are typically below 10 $mg \cdot kg^{-1}$ (Adriano, 1986). It exceeds 100 $mg \cdot kg^{-1}$ which is considered as a trigger level for remediation according to the United States Environmental Protection Agency (US. EPA, 1990).

The PCA multivariate statistical technique helps in distinguishing groups of element categories according to their distribution in solid fractions of the studied soil, obtained from sequential dissolution. PCA combines 7 variables corresponding to different soil phases in 10 row samples, of the MTEs, As, and Sr proportions in each phase compared to the total content in soil (Fig. 5).

In our case, four categories were identified:

1. Category I consists of elements—including As and Cu—that are spread through many of the soil phases including residual, humic-substance, sulfide and oxides as well as organic matter for copper.
2. Category II consists of elements—including Sb, Sn and Cr—mostly found in the residual fraction in a proportion of about 80 to 90%. The remaining amount of Sb and Sn is associated with the humic fraction. Most of the remaining Cr was associated with the soil sulfide fraction. Very low MTEs levels in Category II were bound to the exchangeable, carbonate and Mn-Fe-oxide fractions.
3. Category III consists of elements—including Sr and Cd also bound to the residual phase in slightly lessen proportion (71% and 40% respectively). The remaining Sr and Cd were mostly bound to the exchangeable and carbonates soil fractions (23%–33%). Finally, 12% of the Cd is found in the oxide fraction.

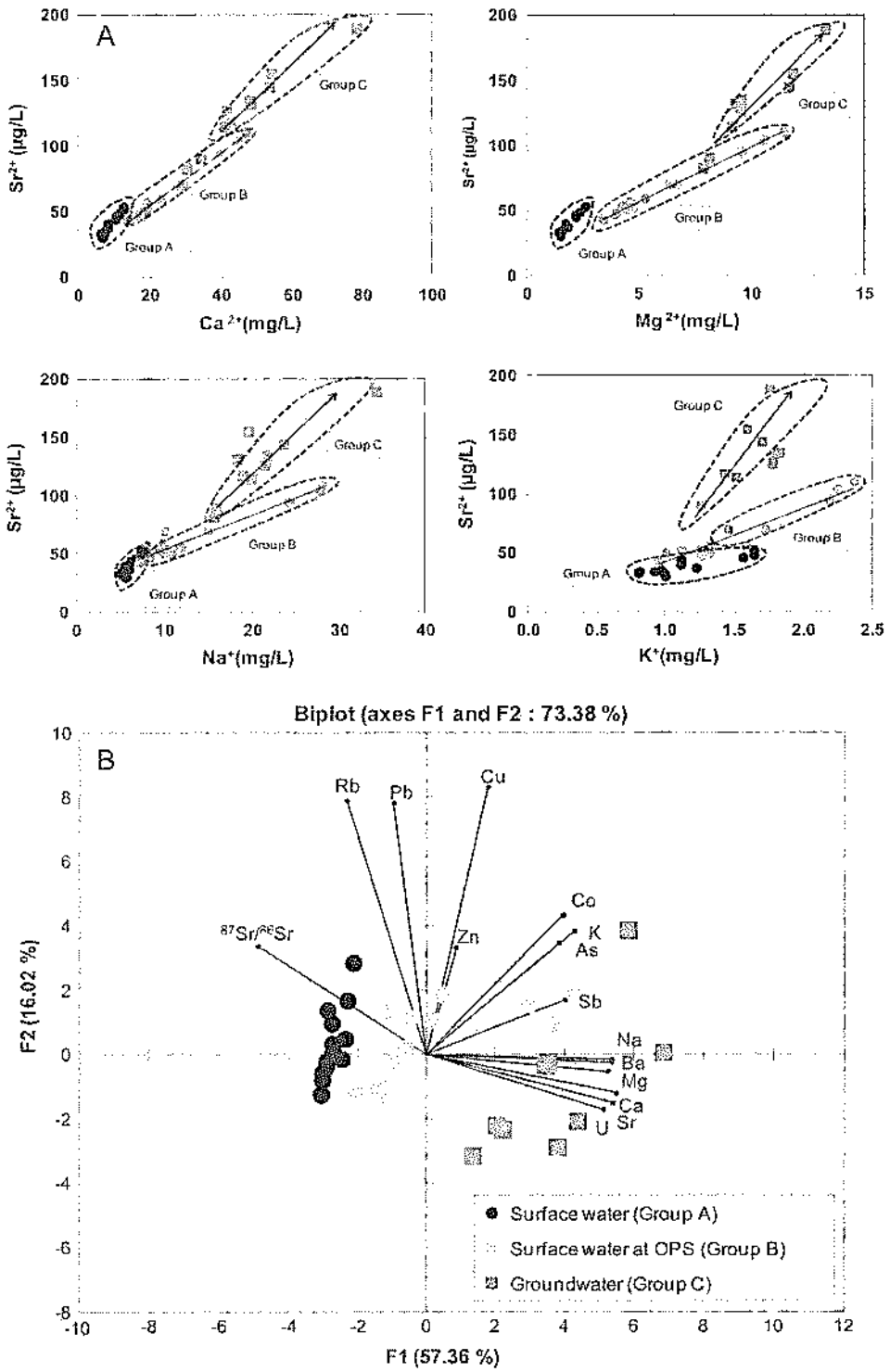

Fig. 2. (A) Binary diagrams of major cations vs. Sr showing the three water groups. (B) Results of the principal component analyses using 15 variables including major elements (Ca, Na, K, Mg), minor elements (Sr, Ba, Rb), trace elements (As, Co, Cu, Zn, Sb, Pb, U) and Sr isotopic ratios ($^{87}Sr/^{86}Sr$).

4. Category IV consists of elements—including Zn, Ni and Co with <50% associated with the residual phase. The fractions associated with sulfide and oxides are important 35–50% respectively. In parallel, high As, Cu, Sr and Cd concentration were observed in the soil H_2O-leachate, and in contrast, the MTEs concentrations showed low concentrations in the leachate.

4.5. Environmental isotopes ($^{87}Sr/^{86}Sr$)

Large isotopic variations were observed in the $^{87}Sr/^{86}Sr$ ratios, decreasing from highly radiogenic values in surface water coming from contaminated groundwater near the reclaimed OPS (Group B) (0.71285–0.71328; Khaska et al., 2015), to much lower ratios of

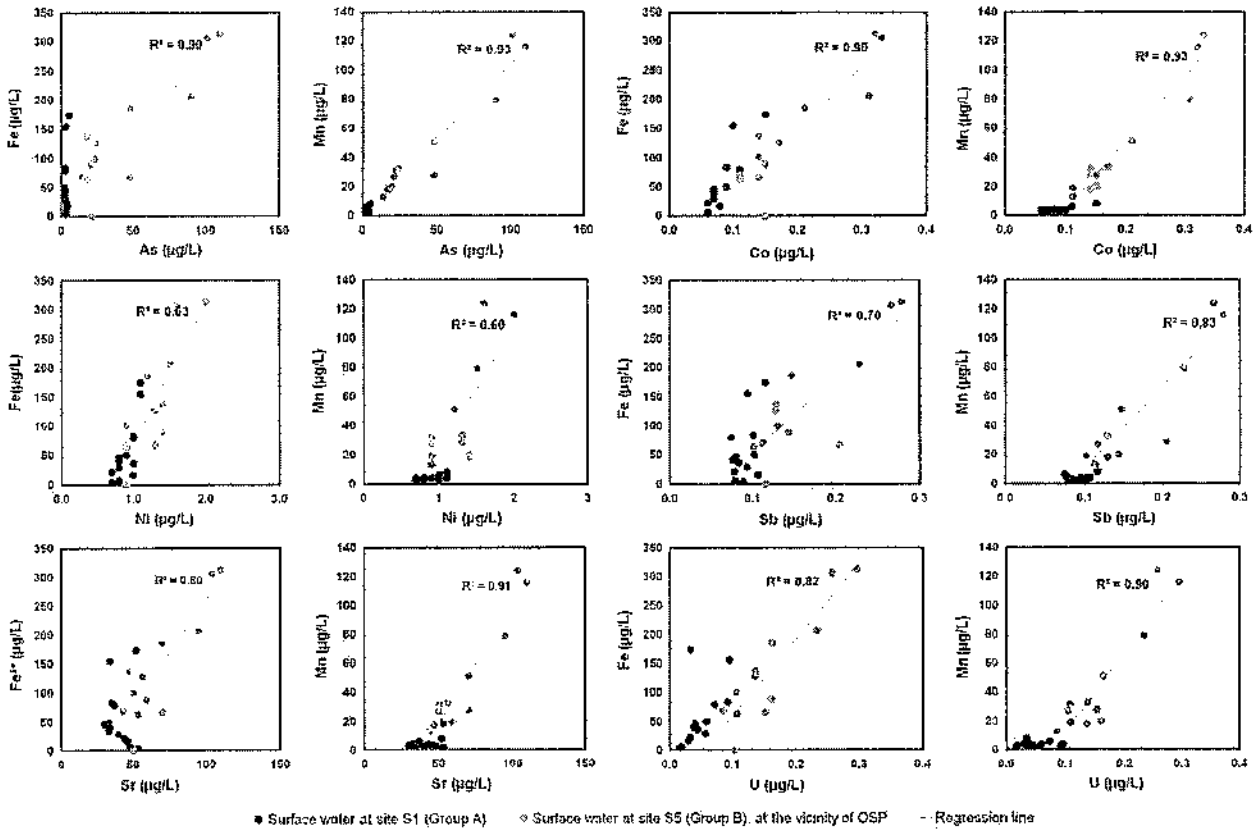

Fig. 3. Evolution of Fe, Mn, As, and MTE concentrations in surface water at the reclaimed OPS site (Group B) compared to incoming surface water, (Group A).

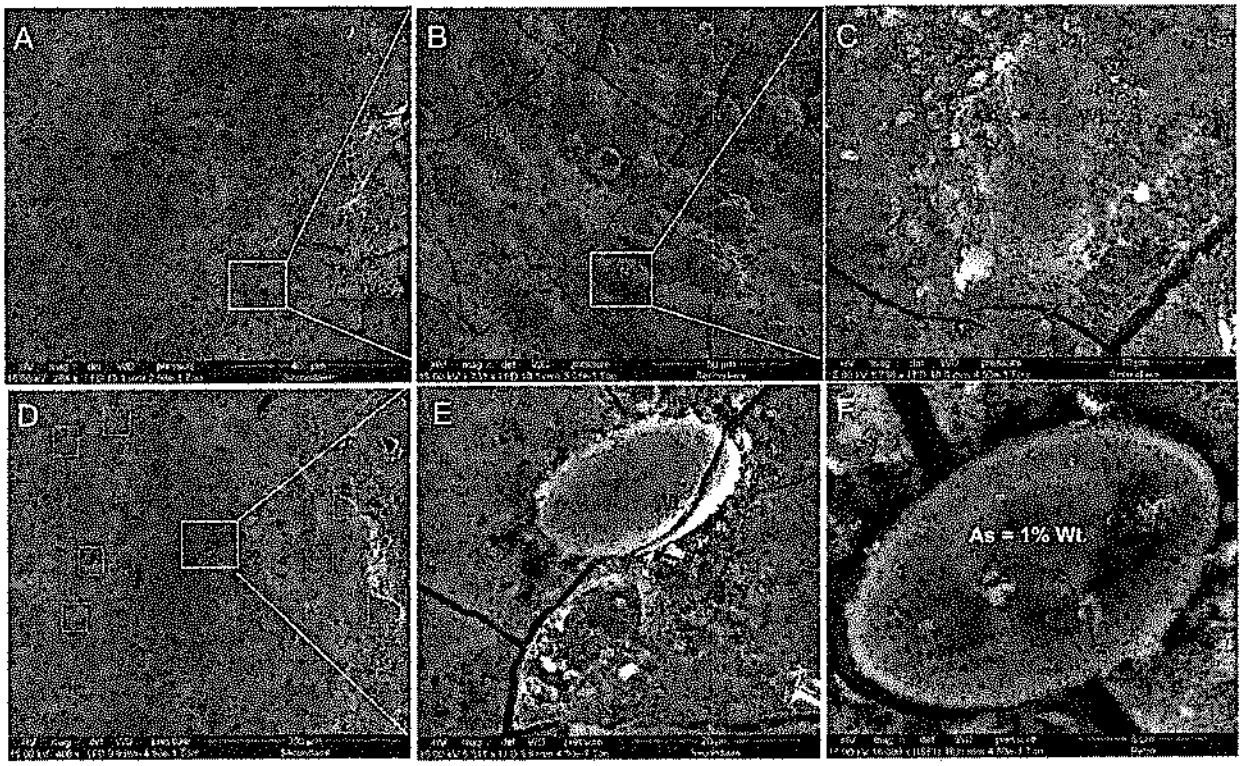

Fig. 4. A is a SEM image of Fe-oxyhydroxide precipitate coating the Orbiel streambed, showing both types of As bearing Fe-oxyhydroxide precipitate. B, and C show a zoom on the abundant nodules on the streambed at site S5 with As content reaching 4.5 wt% (Nodule is marked as "N"). E and F show a zoom on porous diatom silica shells bioadsorbing As bearing Fe-oxyhydroxide. Note the increase of arsenic content in uncoated diatom porous silica before (F) and after bioadsorption of As bearing Fe-oxyhydroxide (E).

Table 3
Analytical results of the sequential extractions carried out on soil sample and compared to the regional pedo-geochemical baseline (INRA, RMQS/GISSOL).

Stage	Fraction	As	Cr	Co	Ni	Cu	Zn	Sr	Cd	Sn	Sb	U	$^{87}Sr/^{86}Sr$
		$\mu g\ kg^{-1}$											
	Sequential extraction												
1	Exchangeable phase	939	250	34	101	801	724	10,648	139	1	20	1	0.71057
2	Carbonates phase	4643	107	816	1013	4069	8344	5573	168	1	10	23	0.71011
3	Fe, Mn oxides phase	14,278	1352	2827	4258	11,086	20,982	1803	109	1	17	144	0.71086
4	Organic matter phase	6103	253	241	617	8002	2558	743	7	0	4	26	0.71346
5	Humic substances phase	33,875	1481	93	319	14,373	226	63	8	321	419	60	0.71117
6	Sulfides phase	17,238	7928	1421	5213	10,857	22,404	2244	57	20	11	173	0.71689
7	Residual phase	26,895	58,565	2179	9523	7211	33,444	51,434	437	4684	2054	2355	0.73086
	Bulk soil	104,117	49,625	8212	28,557	68,152	79,276	54,295	667	2707	1778	1899	
	Soil H_2O leachate	1639	4.7	1.4	20.4	452.5	47.4	368.4	0.4	0.7	16.4	0.5	0.71047
	Pedo-geochemical baseline	31,000	94,000	6400	17,000	31,000	62,000	nd	98	nd	nd	nd	nd

nd: Not determined.

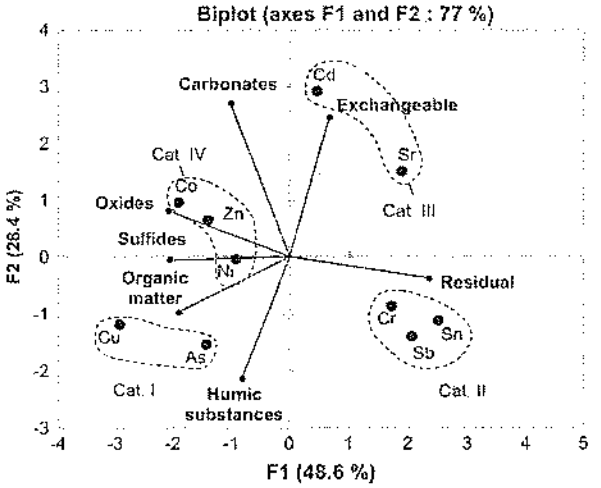

Fig. 5. Results of the principal component analyses combines 7 variables corresponding to different soil phases in 10 row samples of the MTEs, As, and Sr proportions in each phase compared to the total content in soil corresponding to analyzed elements. Based on the PCA analysis four categories were identified.

0.7101 in alluvial soil. Groundwater in the unconfined aquifer downstream of the reclaimed OPS (Group C) showed an intermediate $^{87}Sr/^{86}Sr$ ranging from 0.71058 to 0.71160.

The $^{87}Sr/^{86}Sr$ ratios of the extracted soil solid phases varied significantly between 0.7130 for the residual minerals fraction, and 0.7099 for the carbonate fraction. While, the residual, the sulfide and organic-matter fractions showed significantly contrasted isotopic ratios, most of the other fractions, (oxides, exchangeable and carbonates) have relatively low $^{87}Sr/^{86}Sr$ ratios close to that of carbonate fraction.

The $^{87}Sr/^{86}Sr$ ratio of soil H_2O-leachate was similar to that of oxides, exchangeable and carbonates (Table 3).

4.6. PHREEQC model

The geochemical modeling simulations, performed using the LLNL database, with PHREEQC Interactive 3.4.0 (Parkhurst and Appelo, 1999) supported the results evidenced with Sr isotopes and multivariate statistical approach.

A mixing model, between the labile soil fractions and the average composition of surface water (Group C), was carried out. This model takes into account the physico-chemical parameters of the solutions and the calculated mixing proportions based on $^{87}Sr/^{86}Sr$ mixing diagrams. The results of modeling is presented in Table S3. The results fit well with the observed concentrations MTEs.

5. Discussion

First we discuss the fate of arsenic released from the reclaimed OPS in stream flow.

As precipitates and bioadsorbes on pebbles surface on the streambed.

ESEM measurements of coating streambed indicated the combination of two processes (Fig. 4):

1. Precipitation of ferrous iron (Fe^{2+}) leading to the precipitation of a Fe-oxyhydroxide as observed on all the surfaces of the bedstream.
2. Bioadsorption of As by aquatic microorganisms such as porous diatom silica shells with a higher As adsorption capacity. Zhang et al. (2015) demonstrated the efficiently of the porous diatom silica shells as a sorbent for the removal of arsenic in aqueous solutions, where the bioadsorption capacity reaches 3.5 $mg{\cdot}g^{-1}$ for raw diatoms and 12 $mg{\cdot}g^{-1}$ for modified diatom.

The nodular form observed at pebbles surface in streambed at site S5 results from microorganisms biological activity (e.g. diatoms, bacteria, etc...) coated by a Fe-oxyhydroxide precipitate. Preferential adsorption of As on such organism can explain the higher content in As on nodules surfaces (4 wt% n = 8, SD = 0.6 wt%) compared to the surrounding Fe-oxyhydroxide coating (2 wt% n = 12, SD = 1.1 wt%).

The origin of the As in the precipitated phase was confirmed by the $^{87}Sr/^{86}Sr$ ratios as the $^{87}Sr/^{86}Sr$ ratios of the Fe-oxyhydroxide coating (0.7132) is similar that of surface water collected at Site S5 (0.7130 on average) originating from contaminated groundwater draining the reclaimed OPS (Khaska et al., 2015).

Subsequently, this process contributes to the attenuation of As content in surface water (Khaska et al., 2015). To evaluate the attenuation capacity of the iron hydroxide precipitation we evaluate the As/Fe partitioning coefficient between the Fe-oxyhydroxide and water. According to the kinetics and stochiometry of Fe and As release (Ravenscroft et al., 2009; Smedley and Kinniburgh, 2002), we assume that the partition coefficient of $\frac{As}{Fe}$ between the Fe-oxyhydroxide precipitate and water follows a homogeneous distribution law. This partitioning coefficient, K_d, between the solid and the solution phases is calculated as follows (Ravenscroft et al., 2009):

$$K_d = \frac{\left[\frac{As}{Fe}\right]_{\text{Fe-oxyhydroxide precipitate}}}{\left[\frac{As}{Fe}\right]_{\text{stream water}}}$$

where $\left[\frac{As}{Fe}\right]_{\text{Fe-oxyhydroxide precipitate}}$ is the ratio of As and Fe concentrations sorbed on the Fe-oxyhydroxide film ($\mu g{\cdot}kg^{-1}$) and $\left[\frac{As}{Fe}\right]_{\text{stream water}}$ is the ratio of As and Fe concentrations dissolved in stream water ($\mu g{\cdot}L^{-1}$).

Considering the average As and Fe concentrations of stream water measured between 2006 and 2012 (40 $\mu g \cdot L^{-1}$ and 143 $\mu g \cdot L^{-1}$, respectively) and that of precipitated Fe-oxyhydroxide coatings (31 $g \cdot kg^{-1}$ and 300 $g \cdot kg^{-1}$), a K_d value of 0.36 has been calculated. This value reflects a relatively low As-attenuation capacity of Fe-oxyhydroxide precipitate. In addition, the streambed zone covered with this Fe-oxyhydroxide precipitate is limited to the very close vicinity of the reclaimed OPS, which means that the simultaneous co-precipitation of As is also limited to this zone. As a result, relatively high As concentrations remains in stream flow observed down-gradient of this area.

As and MTEs remaining in solution in the stream water is further reintroduced into the downstream alluvial aquifer.

While part of the arsenic co-precipitates with Fe-oxyhydroxide in the Orbiel streambed near Site S5, most As is transported farther downstream. The average monthly stream flow, recorded upstream of the reclaimed OPS at the GS1 gauging station (3.3–6.8 $m^3 \cdot s^{-1}$), is clearly higher than that measured downstream of the reclaimed OPS at the GS2 gauging station (0.2–5.9 $m^3 \cdot s^{-1}$) (Fig. 6). The loss of flow between GS1 and GS2 ranges from 10% during the wet season up to 90% during the dry season.

This 10–90% stream-flow decrease between GS1 and GS2 plays a major role in As and MTE transfer into the unconfined aquifer downstream of the reclaimed OPS. The surface-water loss may be due to stream-water infiltration into the unconfined aquifer as a result of natural processes, such as the widening of the alluvial plain, or the evolution of the aquifer materials from Variscan basement hard rock at the GS1 station to alluvial sandy loam and detrital material with high permeability and porosity at GS2. This stream-water loss may also be due to anthropogenic processes, such as surface water pumping for agriculture from private wells in the aquifer, or the diversion of stream water into irrigation channels or even groundwater extraction in the close vicinity of the stream

Mixing of surface water and groundwater will impact the latter's quality. The MTE and As input from the infiltrating contaminated surface water into groundwater can be estimated based on stream-flow loss rate. The C_{tot} weighted average of As and MTE concentrations in surface water recharging the aquifer can be estimated as follows:

$$C_{tot} = \frac{(\%\ \text{loss} \times Q_{GS1}) \times \sum C)}{\sum(\%\ \text{loss} \times Q_{GS1})}$$

where % loss is the percentage of stream-flow loss depending upon the sampling period, Q_{GS1} ($m^3 \cdot s^{-1}$) is the stream flow, and C ($\mu g \cdot L^{-1}$) are the As and MTE concentrations in the stream water.

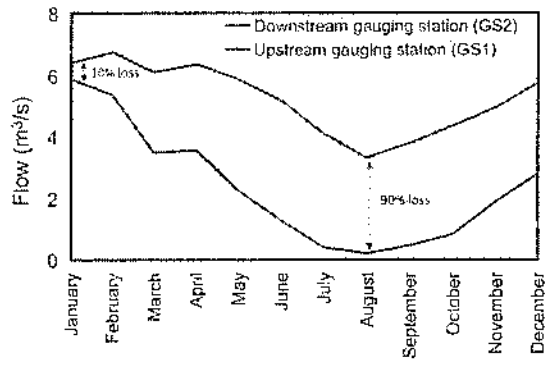

Fig. 6. Monthly average flow at the Lastours gauging station (GS1) from 01/01/2001 to 31/12/2010 and, (2) at the Boudhonnac gauging station (GS2) from 01/01/2001 to present (data from www.hydro.eaufrance.fr).

According to weighted-average calculations, the observed MTEs concentrations in alluvial groundwater, As concentrations excepted, are 2–3 times higher than the calculated concentrations, depending on the considered element. In contrast, the observed As concentrations, lower than the calculated concentrations, suggest a high retention rate of the introduced As in alluvial aquifer by adsorption process and/or oxidation process. The increase in MTEs concentrations suggests that another MTEs source must be considered. Indeed, in binary diagrams of Sr *vs.* MTEs and As (Fig. S3), groundwater, from the downstream unconfined aquifer (Group C) plots between the surface water end member (Group B) and the soil-fraction leachate. This suggests that As and MTEs accumulated in alluvial-plain soil may constitute a possible additional source of these elements in groundwater. In order to define the soil fraction contributing to As and MTEs concentrations in groundwater, we used Sr isotopic data.

Here, we investigate the role of soil in the fate of As and MTE in the groundwater.

Strontium isotopes are suitable tracers for tracking As and MTE transfer in the soil water/groundwater, because of:

1. High Sr concentrations in the different solid-phase fractions of soil, ranging from 0.06 $mg \cdot kg^{-1}$ for the humic-substances fraction to 54 $mg \cdot kg^{-1}$ for the residual fraction;
2. The similar geochemical behavior of Sr and MTE, including As, in most geochemical processes occurring in soil, such as adsorption, sorption, cationic exchange, complexation on clay-humic complexes or reductive dissolution of oxides, and,
3. Contrasting isotopic compositions between different soil fractions that reflect multiple sources of Sr in soil, and multiple processes affecting the As and MTE contents.

The relatively low $^{87}Sr/^{86}Sr$ ratios of the autogenic soil phases represented by carbonate minerals, Fe-Mn oxides, humic substances and exchangeable fractions, compared to surface water, can be explained by the influence of anthropogenic Sr from the reclaimed OPS on soil. Such Sr is characterized by relatively low $^{87}Sr/^{86}Sr$ ratios (0.7122) and its influence on the soil signature is noticeable subsequently flooding periods (Khaska et al., 2015).

Based on the very good correlation between As and Sr as well as between As and MTE (Fig. S2), As and MTE in autogenic soil fractions mainly come from contaminated irrigation water and/or from flooding periods. The similarity of $^{87}Sr/^{86}Sr$ ratios of carbonate minerals, Fe-Mn oxides and exchangeable soil fractions indicates that As and MTE are derived from a single source.

However, the allogenic solid phase fractions such as sulfide minerals and residual crystal minerals come from weathered Variscan crystalline rocks as a detrital phase. The $^{87}Sr/^{86}Sr$ ratios of sulfides and residual crystal mineral fractions are significantly more radiogenic than those of autogenic soil and correspond to the $^{87}Sr/^{86}Sr$ ratios of eroded crystalline rock.

The As and MTE associated with the sulfides and residual crystal minerals in the studied soil further derive from weathered Variscan metasedimentary rock that contains relatively high concentrations of these metals (Demange et al., 2006). Similarly, MTE and As in solid-phase organic matter seem to be of allogenic soil constituents, as the organic-matter fraction has a slightly more radiogenic geochemical and Sr-isotopic signature than the autogenic fraction.

The implication of contaminated soil on the As and MTE contents of groundwater can be tracked by Sr isotopes. In the $^{87}Sr/^{86}Sr$ *vs.* 1/Sr diagram (Fig. 7), groundwater from the unconfined aquifer downstream from the reclaimed OPS (Group C) falls along a water-soil interaction line suggesting the influence of both end members. The most radiogenic end-member is Orbiel stream water affected by contaminated groundwater at the reclaimed OPS (Site S5, group

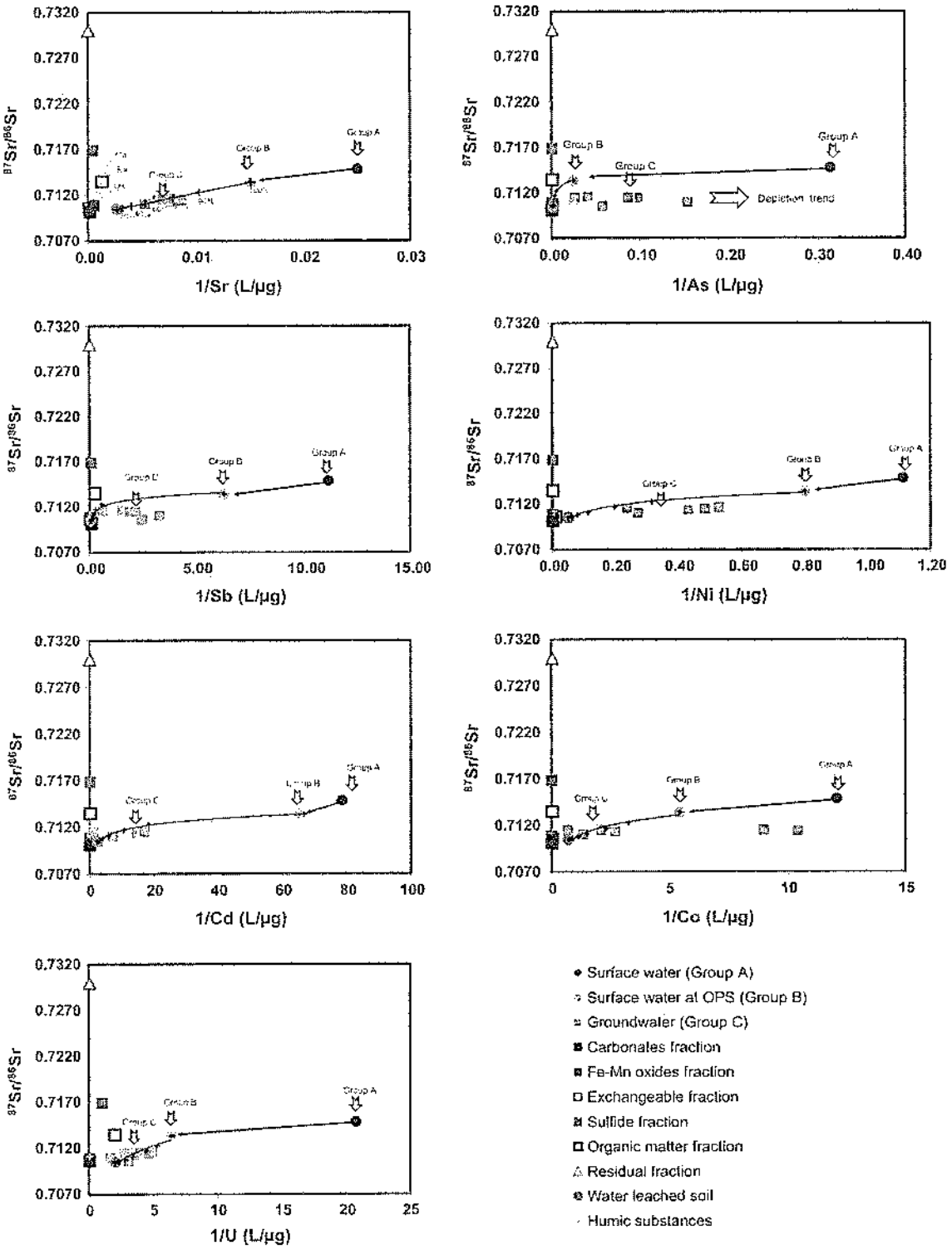

Fig. 7. $^{87}Sr/^{86}Sr$ vs. 1/MTE and Sr (1/µg) mixing diagrams showing a decreasing trend of $^{87}Sr/^{86}Sr$ between contaminated surface water at site S5 and labile alluvial soil. The black arrow illustrate the increase of As and MTEs at site S5 due to OPS influence, the black line represents the mixing between contaminated surface water and the labile soil fractions presented by the soil H_2O leachate reflecting the equilibrium between solid labile fractions and the infiltrated water through soils.

B), with $^{87}Sr/^{86}Sr$ ratios ranging from 0.7128 to 0.7140 (Table 1). The least radiogenic end-member has a $^{87}Sr/^{86}Sr$ ratio similar to those of the autogenic fractions constituting the labile reservoir in the soil, thus suggesting an impact of contaminated soil on the underlying unconfined groundwater. The soil H_2O-leachate was considered as the least radiogenic end-member representing the equilibrium between infiltrated water through soil and labile soil fractions.

Table 4
Percentage of total labile and non-labile fractions of As and MTE extracted in the studied agricultural soil.

MTE	Cr	Co	Ni	Cu	Zn	As	Sr	Cd	Sb
% Carbonates phase/total	0.2	10.7	4.8	7.2	9.4	4.5	7.7	18.2	0.4
% Fe, Mn oxides phase/total	1.9	37.2	20.2	19.7	23.7	13.7	2.5	11.8	0.7
% Exchangeable phase/total	0.4	0.4	0.5	1.4	0.8	0.9	14.7	15.0	0.8
% Humic substances phase/total	2.1	1.2	1.5	25.5	0.3	32.6	0.1	0.9	16.6
Total percentage of labile fraction: (Fe-Mn Oxides, Carbonates, Exchangeable and Humic substance)	5	50	27	54	34	52	25	46	18
% Sulfides phase/total	11	19	25	19	25	17	3	6	0
% Organic matter phase/total	0.4	3	3	14	3	6	1	1	0
% Residual phase/total	84	29	45	13	38	26	71	47	81
Total percentage of Non-labile fraction: (Sulfidic mineral, Residual minerals, and Organic matter)	95	50	73	46	66	48	75	54	82

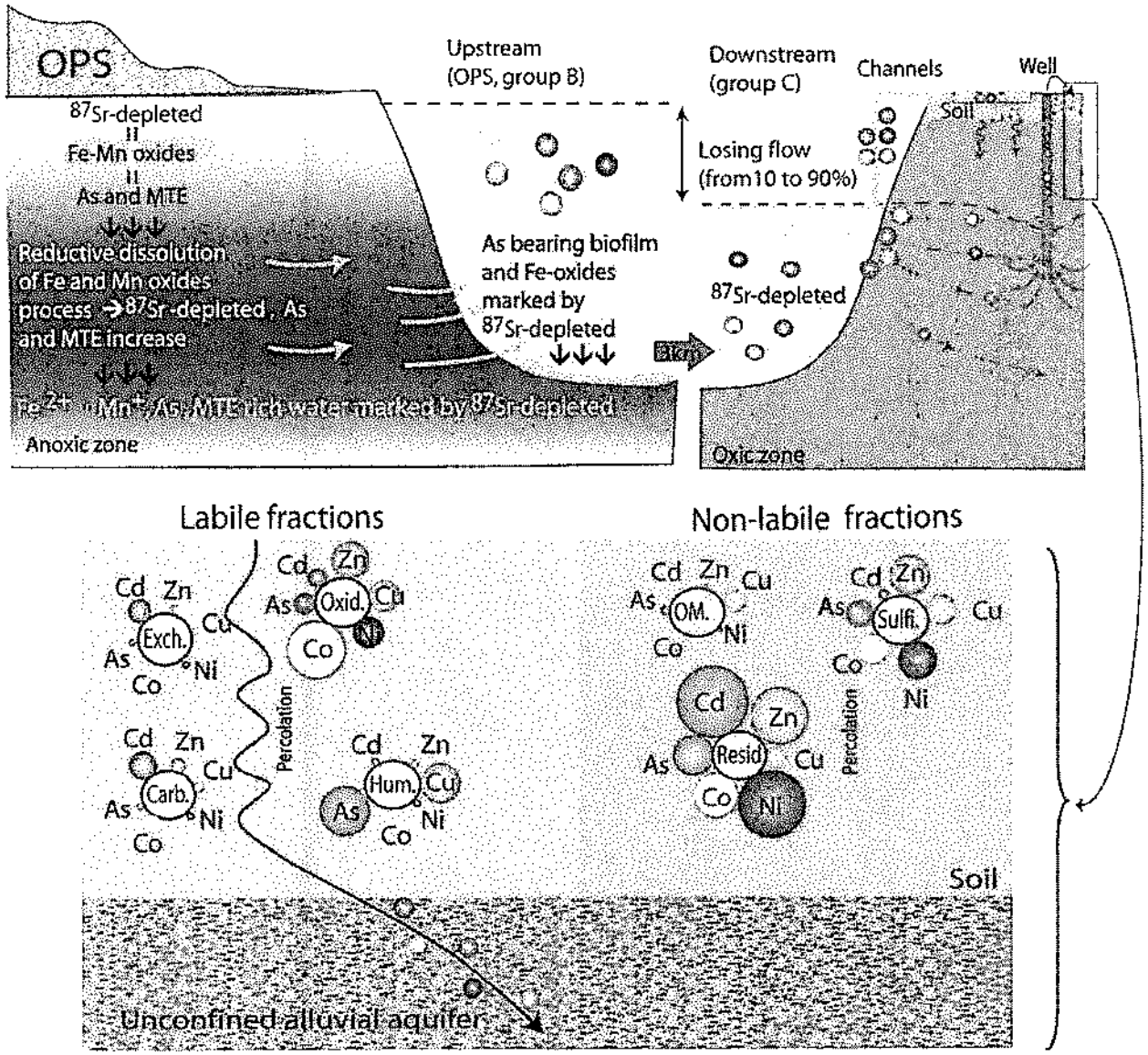

Fig. 8. Conceptual model summarizing the processes and pathways influencing As concentrations in surface and groundwater.

The high $^{87}Sr/^{86}Sr$ ratios of the allogenic fractions (sulfides and residual crystal minerals) compared to those of the autogenic fractions (Fe-Mn oxides, carbonates and exchangeable fractions), confirm the lack of a contribution by allogenic fractions to the As and MTEs content in groundwater. Hence, the allogenic fractions can be described as non-labile in the physico-chemical context of the studied soil. The labile As and MTE fraction constitutes approximately 33% of the total amount of MTEs in soil (Table 4).

Based on a two homogenous components mixing model (Faure, 1986) in the $^{87}Sr/^{86}Sr$ vs. Sr diagram between the soil labile

fractions, as the soil H_2O-leachate, and the Orbiel stream water at site S5 (Fig. 7), the mixing proportion of the soil labile fraction solution can be estimated to be between 25 and 40% in the unconfined groundwater. The calculated proportions of MTEs from the soil labile fraction are in the range of that calculated for Sr (40% for Ni, Cd and 60% for Cd and U) which may suggest a similar geochemical behavior during the transport of these MTEs from agricultural soil to underling groundwater.

However, to support the precision of proportion calculations, complementary experiments on soil-water kinetic equilibrium is required to better define the soil H_2O leachate composition.

The geochemical processes controlling the As and MTEs release into groundwater are controlled by the interactions between the different soil constituents and water percolating in soil, such as irrigation water, effective precipitation or flood water.

The labile soil fraction as indicated by the isotopic approach includes:

1. A carbonate fraction through the dissolution process causing the release of metals sorbed and/or incorporated into the calcite crystal lattice;
2. An exchangeable fraction associated with clay minerals, organic matter or humic substances that may release MTEs through ionic exchange. It is well known that the adsorption/desorption process is pH dependent (e.g., Peters, 2008). High MTEs concentrations are usually associated with alkaline pH in water. Hence, the relatively high pH value observed in the soil promotes the release of As and MTEs into groundwater through effective precipitation (about 250 mm/y in the study area), infiltration of contaminated water during irrigation, and/or flooding events;
3. Iron oxides, from which MTEs releases is also controlled by adsorption/desorption. The high specific-surface area of iron oxides (up to 250–300 $m^2 \cdot g^{-1}$), and its high adsorption capacity (up to 55 $g \cdot kg^{-1}$) make it a privileged component for exchanging other MTEs with soil solution (Driehaus, 2002).

While, the mobilization of MTEs from sulfides can be due to the oxidation processes that release these elements in soil (Moore et al., 1988; Smedley et al., 1996). However, our approach shows that the dissolution of sulfides cannot explain the MTEs release from contaminated soil, as the $^{87}Sr/^{86}Sr$ ratios of the sulfide fraction are significantly higher than the required end-member. This observation is further consolidated by the reducing character of the studied soil. The observed shift in As concentrations, from the mixing curve (Fig. 7), may be explained by retention of As into the alluvial aquifer materials by oxidation and co-precipitation processes. This hypothesis is supported by the very low Fe and Mn concentrations resulting from the oxidizing conditions of the alluvial groundwater where As is adsorbed in such conditions. Moreover, the high redox potential of alluvial groundwater enhance As sorption (Gao et al., 2006). Opposite processes were observed by Hunda et al. (2013) where arsenic mobilization from alluvial soil was observed in relation to decreasing redox potential.

Also, based on the PHREEQC modeling results, the calculated MTEs total concentrations were plotted against the measured MTEs concentrations for comparison. The modelled concentrations fall globally within <16% of variation compared to of the observed data.

Based on these observations a conceptual model of the processes affecting As and MTE transport is constructed.

A conceptual model was developed integrating the results derived from the present study and that of Khaska et al. (2015) (Fig. 8). The hydrodynamic and hydrochemical processes affecting As and MTE transport in the studied hydrological system are summarized below:

1) A reducing zone exists in the aquifer near the reclaimed OPS, which is enriched in As- and MTEs via the reductive dissolution process;
2) Discharge of groundwater down-gradient of the reclaimed OPS, leading to an increase in As and MTE concentrations in surface water;
3) Precipitation of the Fe-oxyhydroxide, with only low partial precipitation (K_d = 0.36) of dissolved As content from the surface water,
4) The contaminated surface water is then reintroduced into the unconfined aquifer farther downgradient of the reclaimed OPS,
5) Release of As and MTEs from the contaminated labile soil fractions linked to carbonate, Fe-Mn oxides and exchangeable sites.

6. Conclusions

We assessed the fate of As and other associated chalcophile MTEs and their transport mechanism in the surface-water/groundwater/soil continuum in a reclaimed mining context. Sr-isotope ratios used as tracers of As and MTEs transfer and their combination with sequential soil-extraction work, have proved that increasing As concentrations in surface water are explained by As released from unconfined groundwater associated with the occurrence of a reducing zone down-gradient of the reclaimed OPS. Such reducing conditions contribute only slightly to the immobilization of As in surface water, where the oxidation of Fe (II) to Fe(III) is confirmed by As–rich Fe-oxyhydroxide precipitate. The major part of As in surface water is reintroduced into the unconfined aquifer downstream of the contamination plume through surface-water infiltration. Study of the $^{87}Sr/^{86}Sr$ ratios identified the soil fractions influencing the underlying groundwater. Moreover, our data show that the mobilization of As and MTEs in contaminated soil varies significantly as a function of the MTEs categories. It varies between 5% for Cr in Category 2, and 52% for As in Category 1. The labile fractions are mainly bound to carbonate, Fe-Mn oxides, and exchangeable and humic substance fractions.

This study, based on an original methodology, has strong implications in characterizing the cycling of MTEs and arsenic in a post-mining context, where pollution by these elements persists even after mine closure. Our study also has led to a better understanding of the key geochemical processes that occur during interactions between groundwater and surface water, and their implications on the fate of As and MTEs. For post-closure management and environmental issues, it is of outstanding importance to determine the origins of pollution (e.g. soils, sediments, tailing dams, runoff, streams, or groundwater) in the local hydrogeological context that was strongly modified during mine exploitation, the different pollutant transfer processes, and the impact of pollutant mobilization on the underlying unconfined aquifer especially when such groundwater is used for irrigation of agricultural products and private vegetable gardens.

Acknowledgements

This research is a part of the ongoing research program «Transdisciplinary approach to environmental risks» funded by the University of Nîmes-CHROME. The authors want to thank the Orbiel Valley inhabitants and Salsigne ancient miners for their warm welcome, informative discussions and their assistance in field for groundwater sampling. Guy Augé and Robert Montanet are particularly thanked for their help during sampling. The authors thank the editor and the two anonymous reviewers for their constructive suggestions to improve the quality of the manuscript.

Appendix A. Supplementary data

Supplementary data associated with this article can be found, in the online version, at https://doi.org/10.1016/j.jhydrol.2018.01.021.

References

Adriano, D.C., 1986. Trace Elements in the Terrestrial Environment. Springer-Verlag, New York.

Aquilina, L., Vergnaud-Ayraud, V., Les Landes, A.A., Pauwels, H., Davy, P., Pételet-Giraud, E., Labasque, T., Roques, C., Chatton, E., Bour, O., Ben Maamar, S., Dufresne, A., Khaska, M., La Salle, C.L.G., Barbecot, F., 2015. Impact of climate changes during the last 5 million years on groundwater in basement aquifers. Sci. Rep. 5, 14132. https://doi.org/10.1038/srep14132.

Aubert, D., Probst, A., Stille, P., 2004. Distribution and origin of major and trace elements (particularly REE, U and Th) into labile and residual phases in an acid soil profile (Vosges Mountains, France). Appl. Geochem. 19, 899–916. https://doi.org/10.1016/j.apgeochem.2003.11.005.

Azcue, J.M., Mudroch, A., Rosa, F., Hall, G.E.M., 1994. Effects of abandoned gold mine tailings on the arsenic concentrations in water and sediments of jack of clubs lake, B.C. Environ. Technol. 15, 669–678. https://doi.org/10.1080/09593339409385474.

Azcue, J.M., Nriagu, J.O., 1995. Impact of abandoned mine tailings on the arsenic concentrations in Moira Lake, Ontario. J. Geochem. Explor. 52, 81–89. https://doi.org/10.1016/0375-6742(94)00032-7.

Bardelli, F., Benvenuti, M., Costagliola, P., Di Benedetto, F., Lattanzi, P., Meneghini, C., Romanelli, M., Valenzano, L., 2011. Arsenic uptake by natural calcite: an XAS study. Geochim. Cosmochim. Acta 75, 3011–3023. https://doi.org/10.1016/j.gca.2011.03.003.

Basu, A., Schreiber, M.E., 2013. Arsenic release from arsenopyrite weathering: insights from sequential extraction and microscopic studies. J. Hazard. Mater. 262, 896–904. https://doi.org/10.1016/j.jhazmat.2012.12.027.

Bauer, M., Blodau, C., 2006. Mobilization of arsenic by dissolved organic matter from iron oxides, soils and sediments. Sci. Total Environ. 354, 179–190. https://doi.org/10.1016/j.scitotenv.2005.01.027.

Berger, G., Boyer, F., Debat, P., Demange, M., Freytet, P., Marchal, J., Mazeas, H., Vautrelle, C., 1993. Notice explicative, Carte géol. France (1/50 000), feuille Carcassonne (1037). BRGM Ed, Orléans.

Burton, D., Bush, T., Johnston, G., Watling, M., Hocking, K., Sullivan, A., Parker, K., 2009. Sorption of Arsenic(V) and Arsenic(III) to schwertmannite. Environ. Sci. Technol. 43, 9202–9207. https://doi.org/10.1021/es902461x.

Campanella, L., D'Orazio, D., Petronio, B.M., Pietrantonio, E., 1995. Proposal for a metal speciation study in sediments. Anal. Chim. Acta 309, 387–393. https://doi.org/10.1016/0003-2670(95)00254-4.

Cary, L., Benabderrazig, H., Elkhattabi, J., Gourcy, L., Parmentier, M., Picot, J., Khaska, M., Laurent, A., Négrel, P., 2014. Tracking selenium in the Chalk aquifer of northern France: Sr isotope constraints. Appl. Geochem. 48, 70–82. https://doi.org/10.1016/j.apgeochem.2014.07.014.

Cary, L., Surdyk, N., Psarras, G., Kavvadakis, I., Chartzoulakis, K., Sandei, L., Guerrot, C., Petitenat, M., Kloppmann, W., 2015. Short term assessment of the dynamics of elements in wastewater irrigated Mediterranean soil and tomato fruits through sequential dissolution and lead isotopic signatures. Agric. Water Manage. 155, 87–99. https://doi.org/10.1016/j.agwat.2015.03.016.

Casentini, B., Hug, S.J., Nikolaidis, N.P., 2011. Arsenic accumulation in irrigated agricultural soils in Northern Greece. Sci. Total Environ. 409, 4802–4810. https://doi.org/10.1016/j.scitotenv.2011.07.064.

Cullen, W.R., Reimer, K.J., 1989. Arsenic speciation in the environment. Chem. Rev. 89, 713–764. https://doi.org/10.1021/cr00094a002.

Demange, M., Pascal, M.L., Raimbault, L., Armand, J., Forette, M.C., Serment, R., Touil, A., 2006. The Salsigne Au-As-Bi-Ag-Cu deposit, France. Econ. Geol. 101, 199–234. https://doi.org/10.2113/gsecongeo.101.1.199.

Deschamps, E., Ciminelli, V.S.T., Höll, W.H., 2005. Removal of As(III) and As(V) from water using a natural Fe and Mn enriched sample. Water Res. 39, 5212–5220. https://doi.org/10.1016/j.watres.2005.10.007.

Deuel, L.E., Swoboda, A.R., 1972. Arsenic solubility in a reduced environment. Soil Sci. Soc. Am. J. 36, 276–278. https://doi.org/10.2136/sssaj1972.03615995003600020032x.

Dousova, B., Buzek, F., Rothwell, J., Krejcova, S., Lhotka, M., 2012. Adsorption behavior of arsenic relating to different natural solids: Soils, stream sediments and peats. Sci. Total Environ. 433, 456–461. https://doi.org/10.1016/j.scitotenv.2012.06.062.

Driehaus, W., 2002. Arsenic removal – experience with the GEH process in Germany. Water Sci. Technol. Water Supply 2, 275–280.

Faure, G., 1986. Principles of Isotope Geology, second ed.

Feng, Q., Zhang, Z., Chen, Y., Liu, L., Zhang, Z., Chen, C., 2013. Adsorption and desorption characteristics of arsenic on soils: kinetics, equilibrium, and effect of Fe(OH)3 colloid, H2SiO3 Colloid and phosphate. Proc. Environ. Sci. 18, 26–36. https://doi.org/10.1016/j.proenv.2013.04.005.

Gao, S., Goldberg, S., Herbel, M.J., Chalmers, A.T., Fujii, R., Tanji, K.K., 2006. Sorption processes affecting arsenic solubility in oxidized surface sediments from Tulare Lake Bed, California. Chem. Geol. 228, 33–43. https://doi.org/10.1016/j.chemgeo.2005.11.017.

García-Sánchez, A., Alvarez Ayuso, E., 2003. Arsenic in soils and waters and its relation to geology and mining activities (Salamanca Province, Spain). J. Geochem. Explor. 80, 69–79. https://doi.org/10.1016/S0375-6742(03)00183-.

Gleyzes, C., Tellier, S., Astruc, M., 2002. Fractionation studies of trace elements in contaminated soils and sediments: a review of sequential extraction procedures. Trends Anal. Chem. 21, 451–467. https://doi.org/10.1016/S0165-9936(02)00603-9.

Guan, X., Ma, J., Dong, H., Jiang, L., 2009. Removal of arsenic from water: effect of calcium ions on As(III) removal in the KMnO4-Fe(II) process. Water Res. 43, 5119–5128. https://doi.org/10.1016/j.watres.2009.12.034.

Hundal, H.S., Singh, K., Singh, D., Kumar, R., 2013. Arsenic mobilization in alluvial soils of Punjab, North-West India under flood irrigation practices. Environ. Earth Sci. 69, 1637–1648. https://doi.org/10.1007/s12665-012-1989-y.

Kabata-Pendias, A., 2004. Soil-plant transfer of trace elements – an environmental issue. Geoderma 122, 143–149. https://doi.org/10.1016/j.geoderma.2004.01.004.

Kelderman, P., Osman, A.A., 2007. Effect of redox potential on heavy metal binding forms in polluted canal sediments in Delft (The Netherlands). Water Res. 41, 4251–4261. https://doi.org/10.1016/j.watres.2007.05.058.

Khaska, M., Le Gal La Salle, C., Verdoux, P., Boutin, R., 2015. Tracking natural and anthropogenic origins of dissolved arsenic during surface and groundwater interaction in a post-closure mining context: isotopic constraints. J. Contam. Hydrol. 177–178, 122–135. https://doi.org/10.1016/j.jconhyd.2015.03.003.

Li, X., Thornton, I., 2001. Chemical partitioning of trace and major elements in soils contaminated by mining and smelting activities. Appl. Geochem. 16, 1693–1706. https://doi.org/10.1016/S0883-2927(01)00068-8.

Matschullat, J., 2000. Arsenic in the geosphere – a review. Sci. Total Environ. 249, 297–312. https://doi.org/10.1016/S0048-9697(99)00524-0.

McArthur, J.M., Ravenscroft, P., Safiulla, S., Thirlwall, M.F., 2001. Arsenic in groundwater: testing pollution mechanisms for sedimentary aquifers in Bangladesh. Water Resour. Res. 37, 109–117. https://doi.org/10.1029/2000WR900270.

Moore, J.N., Ficklin, W.H., Johns, C., 1988. Partitioning of arsenic and metals in reducing sulfidic sediments. Environ. Sci. Technol. 22, 432–437. https://doi.org/10.1021/es00169a011.

Muehe, E.M., Scheer, L., Daus, B., Kappler, A., 2013. Fate of arsenic during microbial reduction of biogenic versus abiogenic As-Fe(III)-mineral coprecipitates. Environ. Sci. Technol. 47, 8297–8307. https://doi.org/10.1021/es400801z.

Mukherjee, A., Bhattacharya, P., Savage, K., Foster, A., Bundschuh, J., 2008a. Distribution of geogenic arsenic in hydrologic systems: controls and challenges. J. Contam. Hydrol. 99, 1–7. https://doi.org/10.1016/j.jconhyd.2008.04.002.

Mukherjee, A., von Brömssen, M., Scanlon, B.R., Bhattacharya, P., Fryar, A.E., Hasan, M.A., Ahmed, K.M., Chatterjee, D., Jacks, G., Sracek, O., 2008b. Hydrogeochemical comparison and effects of overlapping redox zones on groundwater arsenic near the Western (Bhagirathi sub basin, India) and Eastern (Meghna sub-basin, Bangladesh) margins of the Bengal Basin. J. Contam. Hydrol. 99, 31–48. https://doi.org/10.1016/j.jconhyd.2007.10.005.

Négrel, P., Petelet-Giraud, E., 2005. Strontium isotopes as tracers of groundwater-induced floods: the Somme case study (France). J. Hydrol. 305, 99–119. https://doi.org/10.1016/j.jhydrol.2004.08.031.

Parkhurst, D.J., Appelo, C.A.J., 1999. User's guide to PHREEQC (Version 2) – a computer program for speciation, batch-reaction, one dimensional transport, and inverse geochemical calculations. Water-Resour. Invest. Rep.

Pennisi, M., Bianchini, G., Kloppmann, W., Muti, A., 2009. Chemical and isotopic (B, Sr) composition of alluvial sediments as archive of a past hydrothermal outflow. Chem. Geol. 266, 123–134. https://doi.org/10.1016/j.chemgeo.2009.05.017.

Peters, S.C., 2008. Arsenic in groundwaters in the Northern Appalachian Mountain belt: a review of patterns and processes. J. Contam. Hydrol. 99, 8–21. https://doi.org/10.1016/j.jconhyd.2008.04.001.

Pin, C., Joannon, S., Bosq, C., Le Fevre, B., Gauthier, P.J., 2003. Precise determination of Rb, Sr, Ba, and Pb in geological materials by isotope dilution and ICP-quadrupole mass spectrometry following selective separation of the analytes. J. Anal. At. Spectrom. 18, 135–141. https://doi.org/10.1039/b211833e.

Polizzotto, M.L., Harvey, C.F., Li, G., Badruzzman, B., Ali, A., Newville, M., Sutton, S., Fendorf, S., 2008. Solid-phases and desorption processes of arsenic within Bangladesh sediments. Chem. Geol. 228, 97–111. https://doi.org/10.1016/j.chemgeo.2005.11.026.

Postma, D., Jessen, S., Hue, N.T.M., Duc, M.T., Koch, C.B., Viet, P.H., Nhan, P.Q., Larsen, F., 2010. Mobilization of arsenic and iron from Red River floodplain sediments, Vietnam. Geochim. Cosmochim. Acta 74, 3367–3381. https://doi.org/10.1016/j.gca.2010.03.021.

Ravenscroft, P., Brammer, H., Richards, K., 2009. Arsenic Pollution: A Global Synthesis. John Wiley & Sons. 10.1002/9781444308785.

Robertson, F.N., 1989. Arsenic in ground-water under oxidizing conditions, south-west United States. Environ. Geochem. Health 11, 171–185. https://doi.org/10.1007/BF01758685.

Román-Ross, G., Cuello, G.J., Turrillas, X., Fernández-Martínez, A., Charlet, L., 2006. Arsenite sorption and co-precipitation with calcite. Chem. Geol. 233, 328–336. https://doi.org/10.1016/j.chemgeo.2006.04.007.

Smedley, P.L., Edmunds, W.M., Pelig-Ba, K.B., 1996. Mobility of arsenic in groundwater in the Obuasi gold-mining area of Ghana: some implications for human health. Geol. Soc. London Spec. Publ. 113, 163–181. https://doi.org/10.1144/GSL.SP.1996.113.01.13.

Smedley, P.L., Kinniburgh, D.G., 2002. A review of the source, behaviour and distribution of arsenic in natural waters. Appl. Geochem. 17, 517–568. https://doi.org/10.1016/S0883-2927(02)00018-5.

Smith, A.H., 2002. Arsenic epidemiology and drinking water standards. Science (80-.). 296, 2145–2146. https://doi.org/10.1126/science.1072896.

So, H.U., Postma, D., Jakobsen, R., Larsen, F., 2008. Sorption and desorption of arsenate and arsenite on calcite. Geochim. Cosmochim. Acta 72, 5871–5884. https://doi.org/10.1016/j.gca.2008.06.013.

Song, S., Lopez-Valdivieso, A., Hernandez-Campos, D.J., Peng, C., Monroy-Fernandez, M.G., Razo-Soto, I., 2006. Arsenic removal from high-arsenic water by enhanced coagulation with ferric ions and coarse calcite. Water Res. 40, 364–372. https://doi.org/10.1016/j.watres.2005.11.045.

Stumm, W., Morgan, J., 1996. Aquatic Chemistry. A Wiley-Interscience.

Tessier, A., Campbell, P.G.C., Bisson, M., 1979. Sequential extraction procedure for the speciation of particulate trace metals. Anal. Chem. 51, 844–851. https://doi.org/10.1021/ac50043a017.

Teutsch, N., Erel, Y., Halicz, L., Banin, A., 2001. Distribution of natural and anthropogenic lead in Mediterranean soils. Geochim. Cosmochim. Acta 65, 2853–2864. https://doi.org/10.1016/S0016-7037(01)00637-X.

US. EPA, 1990. United States Environmental Protection Agency (U.S. EPA): 1990, Record of Decision (ROD) Abstract ROD Number: EPA/ROD/R08-90/028 ROD Date: 03/30/90 Site: Whitewood Creek, EPA ID Number: SDD980717136, Location:Whitewood, SD. Operable Unit: 01 Environmental.

Welch, A.H., Lico, M.S., 1998. Factors controlling As and U in shallow ground water, southern Carson Desert, Nevada. Appl. Geochem. 13, 521–539. https://doi.org/10.1016/S0883-2927(97)00083-8.

WHO, 1996. Guidelines for Drinking-Water Quality – Second Edition – Volume 2 – Health Criteria and Other Supporting Information. WHO 2, 15.

Xie, X., Ellis, A., Wang, Y., Xie, Z., Duan, M., Su, C., 2009. Geochemistry of redox-sensitive elements and sulfur isotopes in the high arsenic groundwater system of Datong Basin, China. Sci. Total Environ. 407, 3823–3835. https://doi.org/10.1016/j.scitotenv.2009.01.041.

Yokoyama, Y., Tanaka, K., Takahashi, Y., 2012. Differences in the immobilization of arsenite and arsenate by calcite. Geochim. Cosmochim. Acta 91, 202–219. https://doi.org/10.1016/j.gca.2012.05.022.

Zhang, J., Ding, T., Zhang, Z., Xu, L., Zhang, C., 2015. Enhanced adsorption of trivalent arsenic from water by functionalized diatom silica shells. PLoS One 10, e0123395. https://doi.org/10.1371/journal.pone.0123395.

Zheng, Y., Stute, M., Van Geen, A., Gavrieli, I., Dhar, R., Simpson, H.J., Schlosser, P., Ahmed, K.M., 2004. Redox control of arsenic mobilization in Bangladesh groundwater. Appl. Geochem. 19, 201–214. https://doi.org/10.1016/j.apgeochem.2003.09.007.